AIP | Applied Physics Letters

Atomic transport and integrity of Al_2O_3 (2.0 nm)∕HfO_2 (2.5 nm) gate stacks on Si

L. Miotti, R. P. Pezzi, M. Copel, C. Krug, and I. J. R. Baumvol

Citation: Applied Physics Letters **90**, 052913 (2007); doi: 10.1063/1.2437708
View online: http://dx.doi.org/10.1063/1.2437708
View Table of Contents: http://scitation.aip.org/content/aip/journal/apl/90/5?ver=pdfcov
Published by the AIP Publishing

APPLIED PHYSICS LETTERS **90**, 052913 (2007)

Atomic transport and integrity of Al_2O_3(2.0 nm)/HfO_2(2.5 nm) gate stacks on Si

L. Miotti[a] and R. P. Pezzi
Instituto de Física, Universidade Federal do Rio Grande do Sul, Code Postal 15051, 91501-970 Porto Alegre, Rio Grande do Sul, Brazil

M. Copel
IBM Research Division, T. J. Watson Research Center, P.O. Box 218, Yorktown Heights, New York 10598

C. Krug and I. J. R. Baumvol
CCET, Universidade de Caxias do Sul, Rio Grande do Sul 95070–580, Brazil and Instituto de Física, Universidade do Rio Grande do Sul, CP 15051, Porto Alegre, Rio Grande do Sul 91501–970, Brazil

(Received 15 November 2006; accepted 4 January 2007; published online 2 February 2007)

The integrity of Al_2O_3(2.0 nm)/HfO_2(2.5 nm)/SiO_2(<1 nm)/Si(001) stacks after rapid thermal annealing at temperature up to 1025 °C was investigated. The structures were prepared by atomic layer deposition and atomic transport was accessed by profiling all elements in the system with subnanometric depth resolution, using medium and low energy ion scattering and narrow resonant nuclear reaction profiling. Al migration toward the stack/Si interface, Al loss by desorption from the surface, and Hf transport across the Al_2O_3 film layer toward the outermost surface were observed. The loss of oxygen from the stack is also noticeable, most probably caused by compound dissociation and desorption of oxygen containing species. The possible detrimental effects on device electrical properties of the observed presence of Hf at the outermost surface of the dielectric stack and of Al at the dielectric/Si interface are discussed. © *2007 American Institute of Physics*. [DOI: 10.1063/1.2437708]

In order to pursue with the downscaling of Si-based ultralarge scale integration (ULSI) technology, several materials holding dielectric constant higher than that of silicon oxide were proposed as gate dielectric replacements for metal-oxide-semiconductor field effect transistors (MOSFETs).[1,2] The appreciably large dielectric constant, as well as the low density of trapped charges and interfacial electronic states of HfO_2 films on Si, has attracted much attention to this material. However, hafnium oxide films on Si crystallize at relatively low temperatures and do not form effective barriers to the migration of oxidant species and other impurities toward the interface with Si during subsequent postdeposition thermal processing steps of ULSI technology.[2–4] To overcome these difficulties, different Hf-based dielectrics have been proposed for gate dielectric applications, such as Hf silicates and aluminates. However, hafnium silicate films on Si undergo phase separation and crystallization during annealing while hafnium aluminate films on Si present a high density of negative fixed charge.[5,6] As an alternative, it has been proposed that these undesired characteristics can be minimized on well defined, nanoscopic Al_2O_3/HfO_2 stacks on Si, which have the good electrical characteristics of the HfO_2/Si interface and form effective diffusion barriers owing to the topmost Al_2O_3 layer.[7,8] The integration of this kind of gate dielectric in ULSI technology relies, however, on the capability of the stack structure of maintaining its integrity after all thermal processing steps of device fabrication following gate dielectric deposition. In this letter we report on integrity investigations of Al_2O_3/HfO_2 stacks on Si submitted to rapid thermal annealing (RTA) at critical temperatures of MOSFET fabrication processing. Medium energy ion scattering (MEIS),[9] narrow nuclear resonant reaction profiling (NRP),[10] and low energy ion scattering[11] (LEIS) were used to access atomic transport, intermixing, and decomposition of the Al_2O_3/HfO_2 stacks on Si with subnanometric depth resolution.

The Si(001) substrates were wet chemically cleaned and an ultrathin SiO_2 layer (<1 nm) was chemically grown to assist in the initial steps of atomic layer deposition[12] of the $Al_2O_3/HfO_2/Si$ stacks. A 2.5 nm thick HfO_2 layer was grown on the SiO_2/Si substrate using $HfCl_4/H_2O$ precursors and a 2.0 nm Al_2O_3 layer was deposited on top using $Al(CH_3)_3/H_2O$ precursors. The stacks were annealed in ultra high vacuum (UHV) *in situ* in the MEIS analysis chamber for 30 s at temperatures below 850 °C, for 10 s in the range of 850–950 °C, and for 5 s at temperatures above 950 °C. The MEIS spectra were acquired at a scattering angle of 110° with respect to the direction of incidence of a 100 keV H^+ beam aligned with the ⟨100⟩ crystallographic axis of the Si(001) substrate. The outermost surface composition of the $Al_2O_3/HfO_2/SiO_2/Si$ structures were accessed by LEIS using a 2 keV He^+ beam and detecting the scattered ions at 118° with respect to the direction of incidence. Finally, the limitations originated in the overlap of the Al and Si signals in the MEIS spectra[13] were worked out by determining independently the Al profiles and areal densities by NRP, before and after RTA, using the excitation curves of the narrow and isolated resonance at 404.9 keV of the $^{27}Al(p,\gamma)\,^{28}Si$ nuclear reaction at a sample tilt of 50°.

Figure 1 shows the MEIS spectra for the $Al_2O_3/HfO_2/SiO_2/Si$ structures, as prepared and after RTA at 950, 1000, and 1025 °C. For clearness, the spectra obtained after annealing at lower temperatures are not shown in Fig. 1. The ticks in the top axis of Fig. 1 indicate the calcu-

---

[a] Electronic mail: miotti@if.ufrgs.br

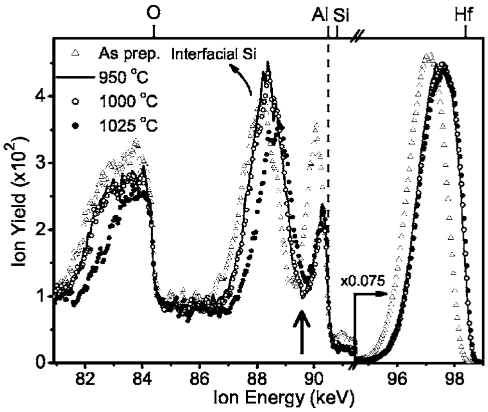

FIG. 1. Medium energy ion scattering spectra obtained in channeling geometry for $Al_2O_3/HfO_2/SiO_2/Si$ stacks as prepared and after rapid thermal annealing at the indicated temperatures. The calculated energies corresponding to H^+ ions scattered by Hf, Si, Al, and O at the sample surface are indicated in the top axis. The vertical arrow around 89.5 keV indicates the notch between the interfacial Si and Al peak after RTA.

lated energy position of H^+ scattered by the different elements at the sample surface. Thus, the Hf peak at 97 keV and the Si peak at 88 keV for the as-prepared sample are at lower energies than those corresponding to ion scattering by these elements at the surface. Thermal annealing is seen to shift the Hf peak to higher energies, indicating the presence of Hf atoms in regions closer to the surface. This may be due to Hf migration into the Al_2O_3 layer, or to partial reduction of the Al_2O_3 layer thickness, or to both. The small increase of the energy width of the Hf peak can be attributed to the spreading of the Hf depth distribution or to an increase of the film roughness. The peak around 90 keV in the MEIS spectrum of Fig. 1 for the as-prepared sample corresponds to Al at the surface of the sample, while the peak around 88 keV is associated with Si in the subnanometric SiO_2 interlayer and in the first few atomic layers of the Si substrate (interfacial Si peak in Fig. 1). The position of the high energy edge (vertical dashed line) of the Al signal, corresponding to Al in the top layer of the structure, does not change after RTA, whereas the reduction of the area of the Al signal reveals its lost from the top layer. The latter effect can be due to desorption of dissociated Al containing compounds[14,15] and/or migration of Al to deeper layers of the stack through the HfO_2 layer toward the dielectric/Si interface. RTA also promoted a shift of the interfacial Si peak to higher energies, as well as a reduction of the width of the oxygen signal caused by desorption of oxygen containing species.[14–16]

In Fig. 2(a) are plotted the Hf and O areal densities and the areal density of Al in the top layer of the structure versus RTA temperature, normalized to their values prior to annealing. Al areal densities in the top layer of the structures were calculated by integrating the area under the peak around 90 keV, without the contribution of the peak region overlapped by the interfacial Si peak. Therefore, the Al data in this plot are rough estimations of the Al areal densities in the samples. Figure 2(b) shows the energy shift of the center of the interfacial Si peak and the shift of the high energy edge of the Hf peak. Only a small reduction of the O areal density, owing to H_2O desorption, is observed for annealing at temperatures below 800 °C.[17] Annealing the $Al_2O_3/HfO_2/SiO_2/Si$ structures above 800 °C shifts the Hf peak toward higher energies and reduces the Al areal density,

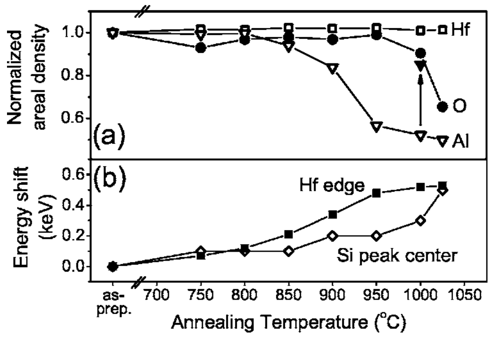

FIG. 2. (a) Normalized Hf (□) and O (●) areal densities in the $Al_2O_3/HfO_2/SiO_2/Si$ stacks and normalized Al (▽) areal density in the top layer of the structure determined by MEIS as functions of the RTA temperature. The normalized Al areal density in the stack annealed at 1000 °C as determined by NRP (▼) is indicated by a vertical arrow. (b) Energy shifts of the high energy edge of the Hf peak (■) and of the center of the interfacial Si peak (◇) in the MEIS spectra as functions of the RTA temperature.

which could be attributed to intermixing of the Al_2O_3 and HfO_2 layers[14] or to partial dissociation of the Al_2O_3 film[14–16] as discussed above. After RTA at 950 and 1000 °C, there is an apparent increase of the intensity of the interfacial Si peak in the corresponding MEIS spectra (Fig. 1), most probably caused by the overlap of the contributions from Al atoms that migrated to near-interface regions and from the interfacial Si peak. Furthermore, RTA at temperatures above 950 °C shifts substantially the interfacial Si peak to higher energies as well as reduces the oxygen areal density (Fig. 2), revealing desorption of oxygen containing species, including AlO, Al_2O,[14–16] as well as SiO from the interfacial layer.[18] The weaker interfacial Si peak observed after RTA at 1025 °C (Fig. 1), as compared to 1000 °C, reveals further dissociation of the interfacial SiO_2 layer, desorbing SiO.

The Al migration into the HfO_2 layer was further investigated using the high elemental and isotopic selectivity of NRP. Figure 3 compares the excitation curves of the $^{27}Al(p,\gamma)\,^{28}Si$ nuclear reaction around the resonance at 404.9 keV for the $Al_2O_3/HfO_2/SiO_2/Si$ structure before and after RTA at 1000 °C. A representation of the sample structure is shown in the inset, where an approximate correspondence between depth in the sample and incident H^+ energy is indicated. The excitation curve for the as-prepared structure shows Al presence only in the top Al_2O_3 film layer, while

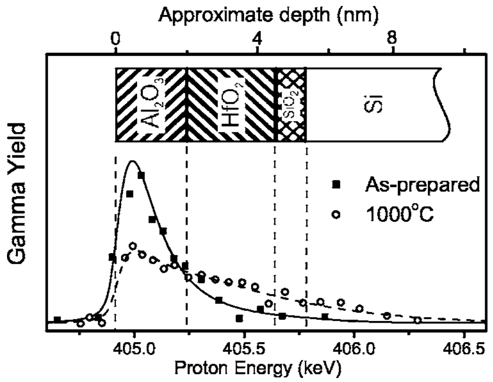

FIG. 3. Excitation curves of the $^{27}Al(p,\gamma)\,^{28}Si$ nuclear reaction near the resonance at 404.9 keV for $Al_2O_3/HfO_2/SiO_2/Si$ stacks as prepared and RTA at 1000 °C. The inset shows a representation of the sample structure, where an approximate correspondence between depth in the sample and scattered H^+ energy is indicated.

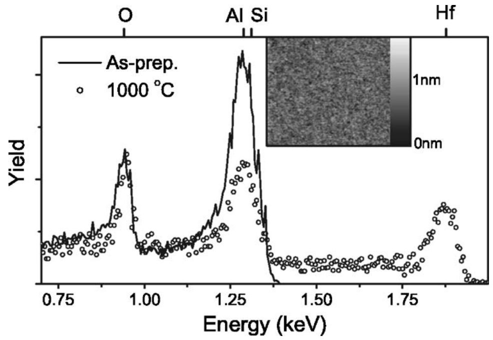

FIG. 4. LEIS spectra of 2 keV He$^+$ ions for $Al_2O_3/HfO_2/SiO_2/Si$ stacks as prepared and after RTA at 1000 °C for 5 s in UHV. The energies corresponding to He$^+$ ions scattered by Hf, Si, Al, and O are indicated in the top axis. The inset shows a 1×1 μm^{-2} AFM image of the sample annealed at 1000 °C.

after RTA a pronounced Al migration into deeper regions of the structure, reaching the interface with the Si substrate, is evident. The shape of the excitation curve after RTA indicates that the Al concentration in the HfO_2 layer after RTA is significantly lower than that in the top layer and that an Al accumulation near the dielectric/Si interface may exist. These facts are corroborated by the notch around 89.5 keV between the interfacial Si peak and Al peak in the MEIS spectrum indicated by a vertical arrow in Fig. 1. The extended tail into the Si substrate region of the annealed sample is possibly an artifact originated in the asymmetry of the resonance in the cross section curve of the nuclear reaction and of the degraded depth resolution in these deeper regions of the sample.[10] Comparing the excitation curves, an overall reduction of the Al areal density after RTA of approximately 15% is estimated, which is much lower than that estimated from MEIS (around 45%). The Al areal density as determined by NRP is quoted in Fig. 2(a) (solid triangle), indicated by a vertical arrow.

Compositional changes of the outermost surface of the stack after RTA at 1000 °C were inspected by LEIS, a method selective to only the first atomic layer at the surface. The spectrum in Fig. 4 for the as prepared structure shows only Al and O signals in the LEIS spectrum, as expected. The presence of a Hf peak in the spectrum for the annealed sample, accompanied by a reduction of the Al signal, indicates that after RTA the outermost surface contains either a mixture of the two oxides, Al_2O_3 and HfO_2, or Hf atoms that migrated to the outermost surface. Nevertheless, similar changes on the LEIS spectra could also result from the formation of pinholes in the Al_2O_3 film during annealing, which would expose the surface of the HfO_2 film layer. Atomic force microscopy (AFM) was used to verify this possibility. The AFM image for the stack sample after RTA at 1000 °C is shown in the inset of Fig. 4, where the small roughness increase (from 0.15 to 0.2 nm) and the absence of pinholes allow us to discard this possibility.

In summary, $Al_2O_3(2.0\ nm)/HfO_2(2.5\ nm)/SiO_2$ (<1 nm)/Si stacks were prepared by atomic layer deposition. Elemental profiling with subnanometric depth resolution was used to access atomic transport and stack integrity following the critical thermal step of dopant activation, performed by RTA at temperatures up to 1025 °C. Starting at 850 °C, RTA induced progressively (1) the transport of Al across the HfO_2 film layer toward the stack/Si interface and (2) Hf transport across the Al_2O_3 film layer toward the outermost surface. These transport and loss processes are accelerated above 950 °C, leading to an effective intermixing of the two layers such that after RTA at 1000 °C, Hf is present at the outermost surface. The loss of oxygen from the stack is also noticeable after RTA at 1000 °C, most probably caused by compound dissociation and desorption of oxygen containing species, including AlO, Al_2O, and SiO from the interfacial region. Even considering that the deposition of the gate electrode prior to dopant activation by RTA would possibly hamper the desorption of these species, it would not affect the atomic transport phenomena observed in the dielectric stack. After dopant activation annealing at 1000 °C, the integrity of the stack is questionable, although an Al-rich region still remains at the surface whereas the interface is Hf rich. Of particular concern for ULSI technology is the arrival of a substantial concentration of Hf atoms to the outermost surface of the stack, as this will change the band alignment of the gate electrode/gate dielectric interface. Along the same lines, the Al doping of the dielectric/Si interface is detrimental, as this will increase the concentration of negative interfacial trapped charge, as well as reduce the carrier mobility in the transistor channel. Investigation is in progress in order to improve the stack integrity by means of annealing in ammonia prior to dopant activation annealing.

The authors acknowledge the financial support provided by the Brazilian agencies CAPES, CNPq, and FAPERGS.

[1] The International Technology Roadmap for Semiconductors, Semiconductor Industry Association, 2004 update (http://public.itrs.net/).
[2] M. Houssa, *High-k Dielectrics* (IOP, London, 2004), p. 123.
[3] R. M. C. de Almeida and I. J. R. Baumvol, Surf. Sci. Rep. **45**, 1 (2003).
[4] G. D. Wilk, R. M. Wallace, and J. M. Anthony, J. Appl. Phys. **89**, 5243 (2001).
[5] S. Monaghan, J. C. Greer, and S. D. Elliotta, J. Appl. Phys. **97**, 114911 (2005).
[6] M. Hiratania, K. Toriib, Y. Shimamotob, and S.-I. Saitob, Appl. Surf. Sci. **216**, 208 (2003).
[7] M. Park, J. Koo, J. Kim, H. Jeon, C. Bae, and C. Krug, Appl. Phys. Lett. **86**, 252110 (2005).
[8] Y. Y. Lebedinskii, A. Zenkevich, E. P. Gusev, and M. Gribelyuk, Appl. Phys. Lett. **86**, 191904 (2005).
[9] R. P. Pezzi, R. M. Wallace, M. Copel, and I. J. R. Baumvol, AIP Conf. Proc. **788**, 571 (2005); M. Copel, IBM J. Res. Dev. **44**, 571 (2000).
[10] C. Driemeier, L. Miotti, R. P. Pezzi, K. P. Bastos, and I. J. R. Baumvol, Nucl. Instrum. Methods Phys. Res. B **249**, 278 (2006).
[11] H. Niehus, W. Heiland, and E. Taglauer, Surf. Sci. Rep. **17**, 213 (1993).
[12] P. D. Kirsch, M. A. Quevedo-Lopez, H.-J. Li, Y. Senzaki, J. J. Peterson, S. C. Song, S. A. Krishnan, N. Moumen, J. Barnett, G. Bersuker, P. Y. Hung, B. H. Lee, T. Lafford, Q. Wang, D. Gay, and J. G. Ekerdt, J. Appl. Phys. **99**, 023508 (2006).
[13] E. P. Gusev, M. Copel, E. Cartier, I. J. R. Baumvol, C. Krug, and M. A. Gribelyuk, Appl. Phys. Lett. **76**, 176 (2000).
[14] L. Miotti, C. Driemeier, F. Tatsch, C. Radtke, and I. J. R. Baumvol, Appl. Phys. Lett. **89**, 012904 (2006).
[15] M. Kundu, N. Miyata, and M. Ichikawa, J. Appl. Phys. **92**, 1914 (2002).
[16] M.-H. Cho, H. S. Chang, Y. J. Cho, D. W. Moon, K.-H. Min, R. Sinclair, S. K. Kang, D.-H. Ko, J. H. Lee, J. H. Gu, and N. I. Lee, Appl. Phys. Lett. **84**, 571 (2004).
[17] C. Driemeier, E. P. Gusev, and I. J. R. Baumvol, Appl. Phys. Lett. **88**, 201901 (2006).
[18] N. Miyata, Y. Morita, T. Horikawa, T. Nabatame, M. Ichikawa, and A. Toriumi, Phys. Rev. B **71**, 233302 (2005).